

## CS2 – MANTA – MULTI-FUNCTIONAL FLAP MECHANISM OFFERING A SECOND DEGREE OF FREEDOM

M. Desmet<sup>1</sup>, J. Vervliet<sup>1</sup>, D. De Wit<sup>1</sup>, R. Seidler<sup>2</sup>, J. Docter<sup>3</sup> & B. Everaert<sup>1</sup>

<sup>1</sup>Asco Industries NV/SA (ASCO)

<sup>2</sup>Deutsches Zentrum fuer Luft und Raumfahrt E.V. (DLR)

<sup>3</sup>Netherlands Aerospace Centre (NLR)

### Abstract

In the frame of project MANTA or “MovAbles for Next generaTion Aircraft”, a Multi-Functional Flap Mechanism (MFFM) concept is developed for a novel wing lay-out which combines load alleviation, roll and high-lift functionalities into one large trailing edge control surface.

The specific flap kinematics allows the multi-functional flap body to be rotated, at high speed, in any given flap position. Next to the concept description, the associated design challenges, aerodynamic effects and demonstration by test of the novel features are addressed towards a functional mechanism.

**Keywords:** flap, multi-functional, novel, kinematics, wing layout

## 1. General introduction

### 1.1 Project MANTA

Project MANTA or “MovAbles for Next generaTion Aircraft” is funded by the Clean Sky 2 Joint Undertaking (CS2JU) and gathers two industrial partners (Fokker Aerostructures B.V. and ASCO), two research centers (NLR and DLR), and a university (Delft University of Technology).

One of the key objectives of the Clean Sky 2 (CS2) programme [1] is to minimize the impact of aviation on the environment through key innovation. A way to achieve this is to increase the effectiveness and enlarge the functionality of the control surfaces of an aircraft. This may lead to a performance increase as it allows the reduction of the structural weight, which has a direct result on the fuel burn and emissions of the aircraft.

By developing and demonstrating novel movable concepts, MANTA contributes to the challenging ambition of the CS2JU to reduce the fuel consumption by 3 to 5%.

### 1.2 Asco Industries NV/SA

ASCO is a world class supplier of high lift structures, complex mechanical assemblies and major functional components [2].

In partnership with our customers, the ASCO engineering team continues to develop innovative cutting-edge technology applications with focus on the high-lift mechanisms on the leading and the trailing edge for almost all commercial aircraft platforms.

ASCO is core partner in CS2 Airframe Integrated Technology Demonstrator (ITD) via the MANTA consortium.

In project MANTA, ASCO developed the MFFM concept adding a second degree of freedom (2<sup>nd</sup> DOF) to state-of-the-art flap kinematics. ASCO calculated interface loads for this concept and performed preliminary and detailed design activities. And defined a set of test objectives and requirements for demonstration by test of the novel features.

### 1.3 Deutsches Zentrum fuer Luft und Raumfahrt E.V.

The DLR, the German Aerospace Center, is the research center of Germany for the subjects of aerospace, energy, traffic, digitalization and safety.

One of the main topics of the institute of aerodynamics and flow technology of the DLR hereby covers the research in aircraft aerodynamics, ranging from numerical simulations in aerodynamics and aeroacoustics, to wind tunnel experiments and all the way up to flights tests.

In project MANTA, the DLR provides insight into the aerodynamics of the different movable concepts on the aircraft, analyzing the effectiveness of the approaches and giving loads and moments for the other disciplines.

For the MFFM, the DLR made an initial study on the positioning and constraints for the High-Lift system on the Dassault Aviation (DAV) High-Sweep Business Jet (HSBJ), worked out the possibilities and conditions for the novel wing layout and finally provides computational fluid dynamic (CFD) studies for its static and dynamic use cases.

### 1.4 Netherlands Aerospace Centre

Royal NLR, Netherlands Aerospace Centre, is a leading technological knowledge institute in the field of aerospace in the Netherlands. NLR makes aerospace more sustainable, safer, more efficient, and more effective. NLR is the connecting link between science, industry, and government.

In the MANTA MFFM project, NLR is responsible for the design and build of the test setups.

The biggest challenge in the test design for the MFFM was to account for the changing aero load moments on the flap section while rotating the flap around a curved hinge line at high speed. Furthermore, the test set up allows for wing bending to be simulated during testing.

With its novel test design approach, NLR aims to achieve simplified but realistic loading in the MFFM. The test will be executed by NLR in the near future.

## 2. Objectives

Aim of the MFFM is to reduce the weight of the aircraft by optimizing high-lift performance and by combining more functionalities into one flap body via the mechanism that is chosen to position the flap. Eventually allowing the removal of one or more control surfaces, such as aileron or spoiler. These functionalities may be:

- High-lift function in take-off and landing configuration
- Adaptable to actual aircraft configuration in terms of optimum aircraft performance at actual payload and external conditions
- High rate of extension of the flap (Fowler motion) of about 50% to obtain a high lift coefficient
- Load alleviation on wing root
- Roll Control at low speed (take-off and landing) – requiring larger deflection of control surface in the range of +/- 20degrees (deg)
- Roll Control at mid to high speeds (cruise) – requiring smaller deflections of control surface in the range of +/- 5deg
- Spoiler or air brake function

### 3. Concept development

An alternative flap concept is investigated by Asco starting from the state-of-the-art 'carriage/rear link' system, found on various types of large aircraft. But re-designed and re-connected to allow for a rotation of the flap (up and downwards) in any given flap position.

Studies are based on the DAV HSBJ wing layout (Figure 1), but the principle is also applicable to large passenger aircraft and low sweep wings.

The mechanism concept that allows for the largest flap rotation in any given flap setting, is selected as best candidate because it is the most flexible and combines a maximum number of functionalities.

#### 3.1 Novel wing layout

The novel wing layout shown in Figure 1 consists of

- 1 inboard (INBD) flap – *proven design*
- 1 outboard (OUTBD) flap supported by 3 flap support stations (ST), 1 master station (reacting flap side loads), 2 slave stations and 2 cruise rollers (Figure 2) – *novel multi-functional flap mechanism*
  - To achieve the same high-lift performance as the reference flap, the spanwise length needed to increase to allow for the aileron function at extended flap setting of 25deg.
  - With the larger flap body, a rotation of +/- 15deg in extended flap setting of 25deg is sufficient to guarantee roll control.
- Deletion of separate aileron control surface – *novel design*
- 4 airbrakes (spoilers) – *proven design*
  - No solution was found to integrate air brake and high lift functionalities, spoilers remain separate control surfaces
- 3 slats – *proven design*

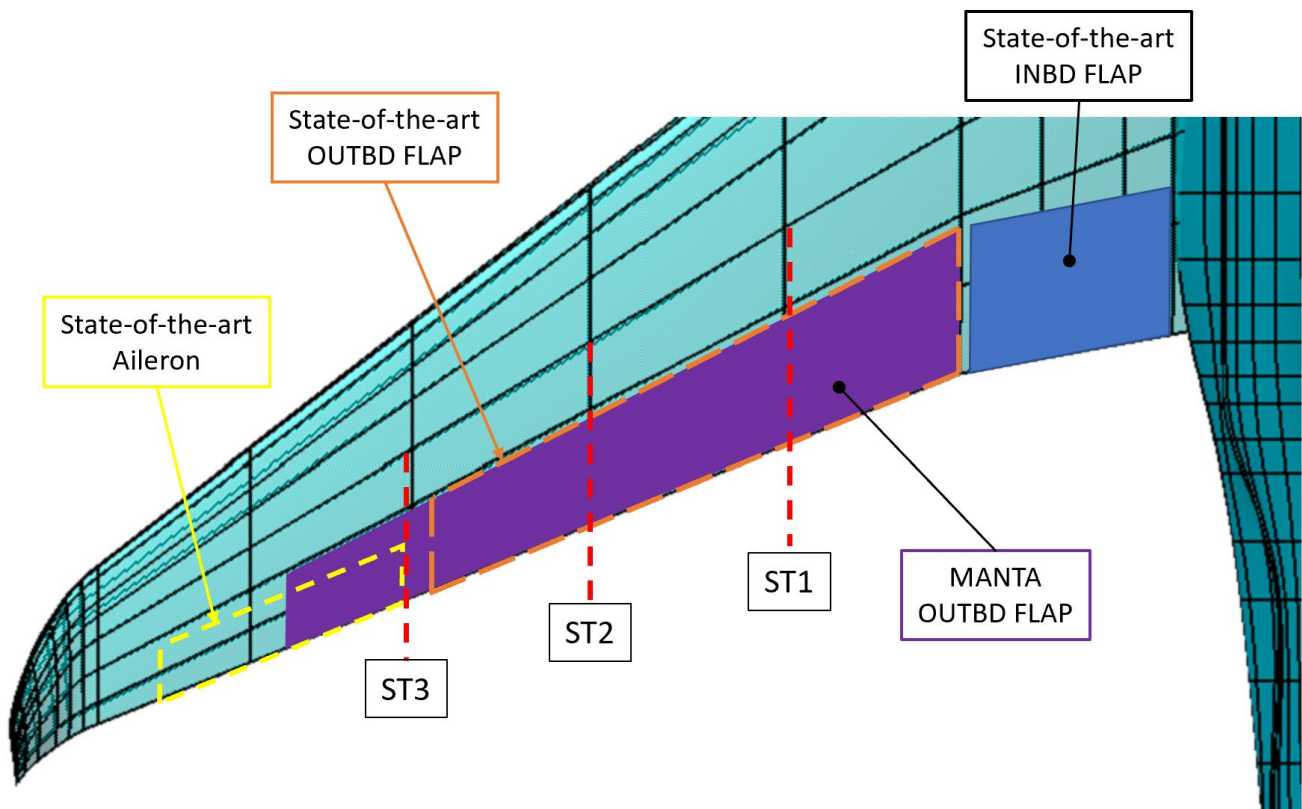


Figure 1 – Novel wing layout (HSBJ)

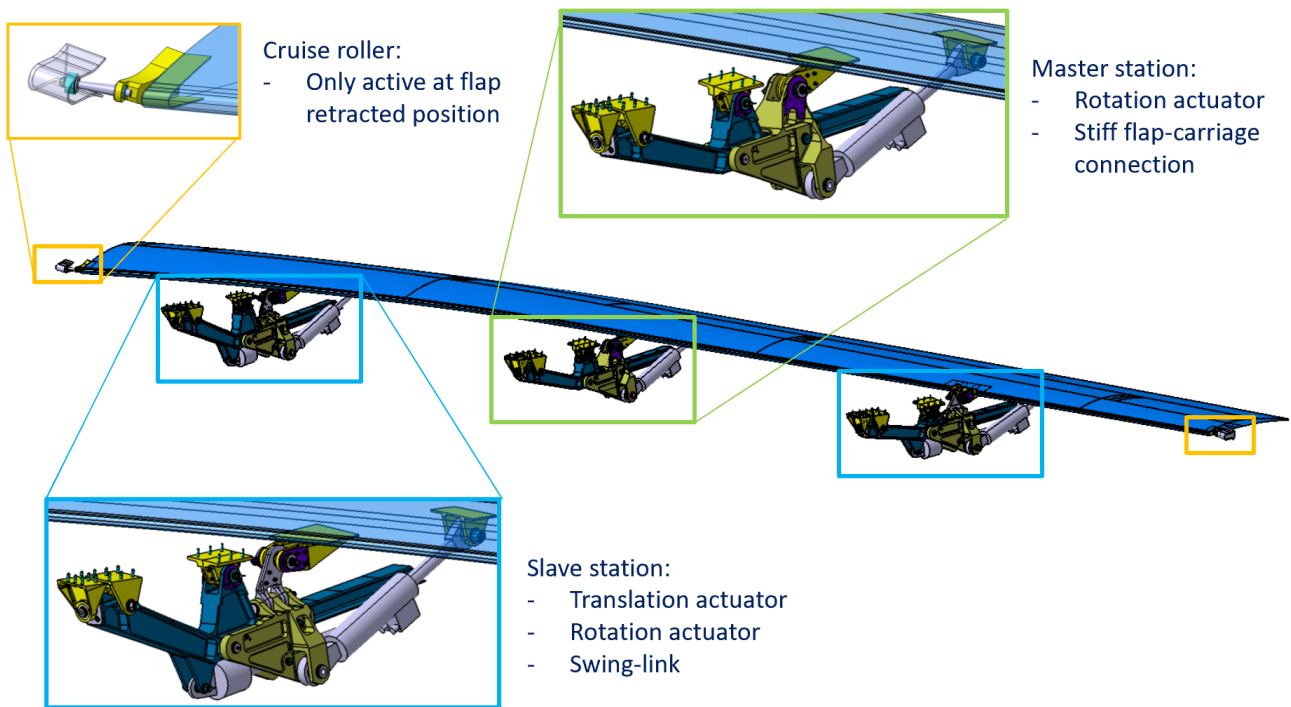


Figure 2 – Novel flap layout (HSBJ)

### 3.2 Selected mechanism concept

Figure 3 visualizes the main common features as well as the innovative change between the state-of-the-art and the MANTA MFFM concepts.

- a track mounted underneath the wing via forward and aft wing attachments – *proven design*
- a carriage that rolls on the track – *proven design*
- an actuator that translates the carriage and flap to any given position on the track – *proven design*
- an actuator that rotates the aft end of the flap +/- 15deg in any flap position and moves together with the carriage – *novel design*

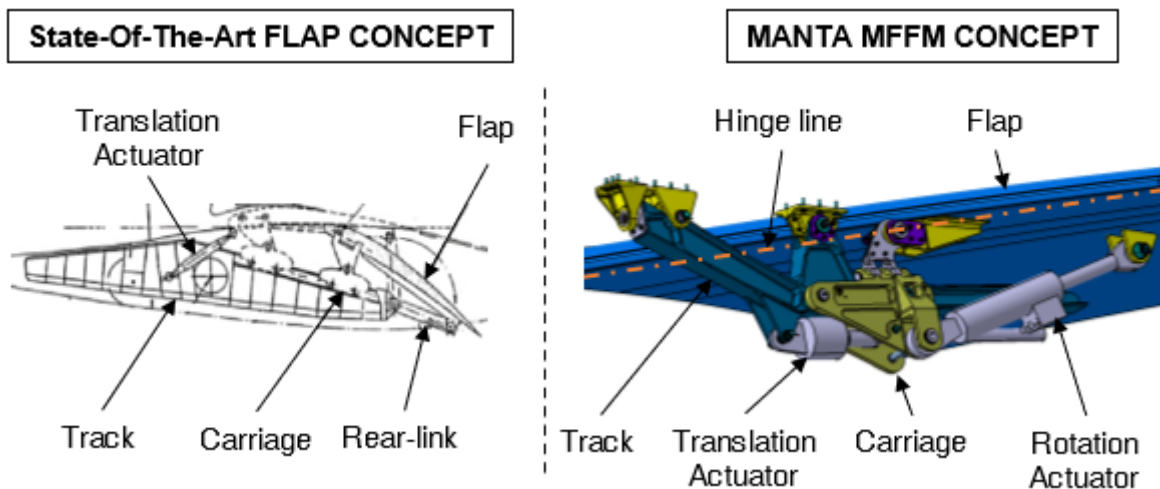


Figure 3 – Track and carriage concept for MFFM

### 3.3 Aero considerations

The current state-of-the-art wing layouts do not allow the integration of a multi-functional flap, since using it as a roll control device would not be possible in fully extended high-lift configuration.

Therefore, for enabling the rolling capabilities in high-lift configuration, the maximum extension angle for high-lift to increase the maximum lift is reduced from 40deg to 25deg. This opens a margin of 15deg in upward and downward deflection for roll control even in fully extended landing configuration.

In a study from DLR, visualized in Figure 4, the effect of the flap size on the roll control efficiency and on the reduced required high-lift deflection angle on the HSBJ is shown. The variable of  $\xi$  here depicts the maximum additional deflection angle, which is needed to achieve roll controllability. The effect on the roll control is even larger, because the spanwise increase of the flap not only increases its affected area, it also shifts the loads to the outer wing and thereby increases the lever arm for the rolling moment.

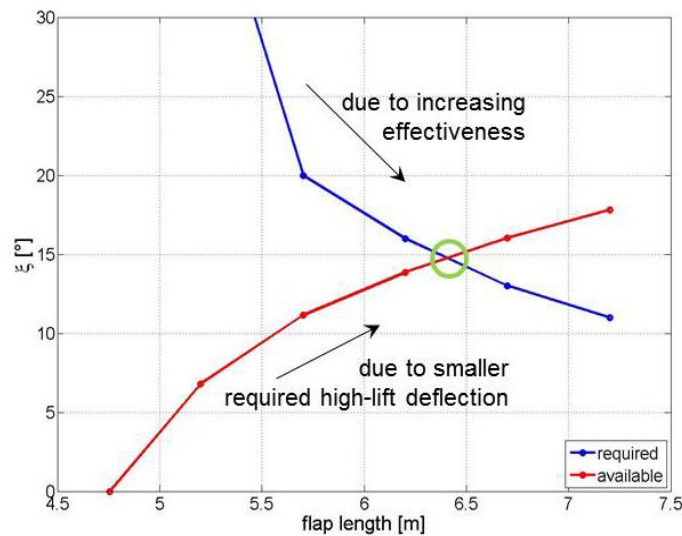


Figure 4 – Optimal flap length for roll control and high-lift for the HSBJ

To compensate the reduction in lift due to the reduced deflection angle in high-lift, the size of the outboard multi-functional flap is increased to achieve the same maximum lift coefficient as in the reference configuration. The greater size of the spanwise outboard flap length also increases the roll efficiency of the flap, it needs less additional deflection angle for rolling and an optimum was found at a flap spanwise length of 6.4m.

With the greater size of the outboard flap, the flap can be fully used for roll control with the same efficiency, even in landing configuration and without compromising the high-lift capabilities.

### 3.4 Aero load input

The wing box is meshed using Finite Elements (FE) such that the wing deflection is realistic, and the aeroelastic bend/twist coupling is captured.

Coupled CFD (Ansys Fluent, S-A Rans) and structural FE (MSC Nastran) analyses are alternately solved until the model converges and the final aero loads on the flap box are computed. These loads are extracted in 52 discrete points on the flap.

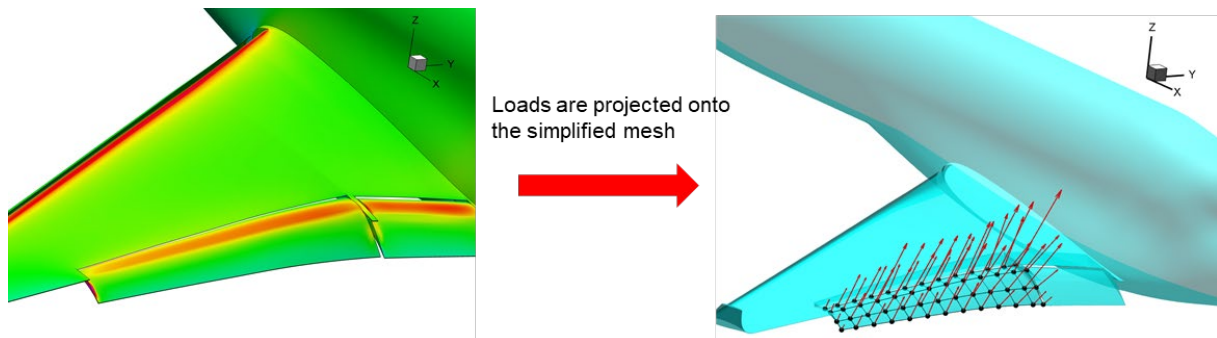


Figure 5 – Load extraction from Flap CFD-FE model

Several aero load cases are generated, by varying following parameters:

- flap position (retracted, extended)
- flap setting (-15°, -5°, 0°, 5°, 15°)
- angle of attack (-2.5°, 0°, 2.5°, 5°)
- roll rate (-50deg/s, +50deg/sec, retracted cases only)

The extracted aero loads are then applied on a Global FE model (MSC Nastran) to derive all internal interface loads. Load cases are defined with and without wing bending. The model is run in intact configuration in limit and ultimate conditions at the different flap positions and settings.

Separate runs are performed with following failures:

- rotation actuator failure: each rotation actuator is alternately taken out, leaving only two rotation actuators to react the hinge moment on the flap.
- translation actuator failure: each translation actuator is alternately taken out, leaving only one translation actuator to react horizontal loading on the flap. The flap will tend to skew.
- carriage jamming: each jamming is alternately considered fixed to the track in horizontal direction (rolling direction). The translation actuators will increase their input load up to their ultimate load or until a skew of 40mm between two stations is observed.

## 4. Design challenges

This section describes how Asco Engineering addressed each of the following design challenges in the final design:

- Optimizing kinematics for high lift, load alleviation and roll control
- Fitting a rotation actuator into a traditional flap support station
- Respecting the aero shape requirements of the large multi-functional flap body in cruise conditions
- Integrating hydraulic tubes that drive the actuators
- Controlling flap skew and maintaining a straight hinge line for flap rotation
- Guaranteeing the aileron function in normal operating and failure conditions – system redundancy
- Moveable fairing kinematics
- Spoiler integration considering flap negative (upwards) rotation

### 4.1 Optimized kinematics

The kinematics is designed not only to align with the defined cruise, landing and take-off flap settings, but in addition to provide the needed space envelope in the system for the rotation actuator integration. Especially the length of the rotation actuator is a main driver for the kinematics. The spanwise position and the angle of the rotation actuator have a significant impact on the reaction loads (amplitude and direction) in the system and its stability.

It is noticed that the rotation actuator mainly tends to rotate outboard during deployment (linked to the HSJB conical flap motion). Therefore, its interface with the carriage is forced to be positioned towards the rear of the carriage and on the outboard side to avoid possible clashes with the carriage, track or translation actuator.

Another main driver on the MANTA kinematics definition is related to the introduction of the cruise rollers. Simulations revealed the need for cruise rollers to keep the flap tips in line with the wing in cruise conditions in order to stay within the desired aero shape. Cruise rollers add a big constraint to the kinematics as they need to be in line with the multi-functional flap hinge line in cruise condition, this is an extra constraint for the MFFM concept. In contrast to current flying flap systems, this is needed as the flap must be able to rotate down- and upwards at any given flap position.

The cruise rollers limit the freedom to optimally position the hinge line as they need to remain in the wing envelope to avoid the need for additional fairings.

On the given wing geometry this constraint drives the hinge line too close to the flap lower skin for a typical forward flap lug integration (see Figure 6 below). Therefore, the hinge line has been moved in front of the flap leading edge as seen in Figure 15.

Having the hinge line in front of the flap has as benefit that the flap leading edge does not move forward significantly when rotating upwards and only limited gaps to the surrounding systems / wing box need to be foreseen.

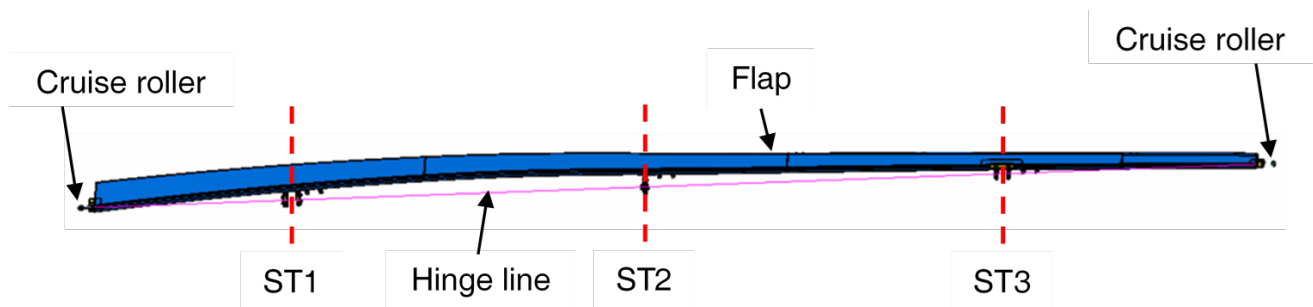


Figure 6 – Hinge line on curved flap

## 4.2 Rotation Actuator (RA)

To actuate the rotation of the flap, both electrical and hydraulic actuators can be used. However, off-the-shelf electrical actuators seem to require more space allocation and have a higher weight. Therefore, a hydraulic actuator is preferred. As explained in chapter 4.1 above, the carriage-RA connection is located on the aft part of the carriage, limiting the freedom of actuator stroke. For the multi-functional flap rotation requirements and available space allocation a suitable hydraulic actuator is selected. The hydraulic tubes, connected to the hydraulic actuator, provide the required pressure (see chapter 4.3 below).

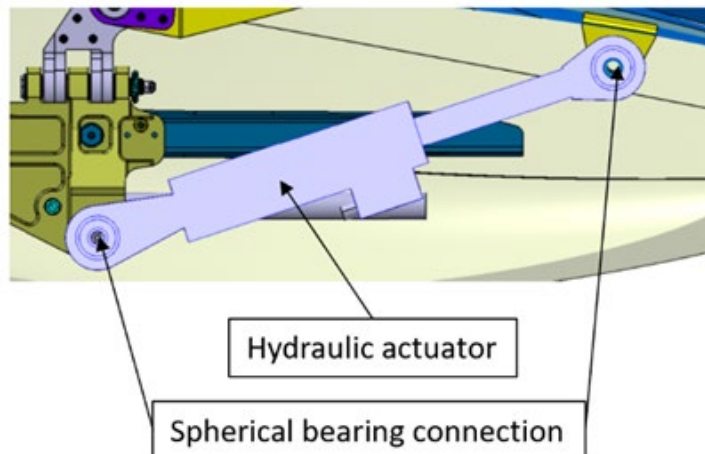


Figure 7 – Rotation actuator Integration

## 4.3 Hydraulic tubing

Attaching a hydraulic actuator to the movable carriage brings a challenge to provide hydraulic pressure for that actuator in any position. Two flexible hoses (Figure 8), attached at one side to the wing and at the other side on the actuator, provide the needed power combined with the capability to follow the carriage movement.

To avoid having cables of more than 1 meter moving uncontrollably in the fairing, a guidance concept is required to force the tubes to follow the desired path. Several options for this guidance will be tested.

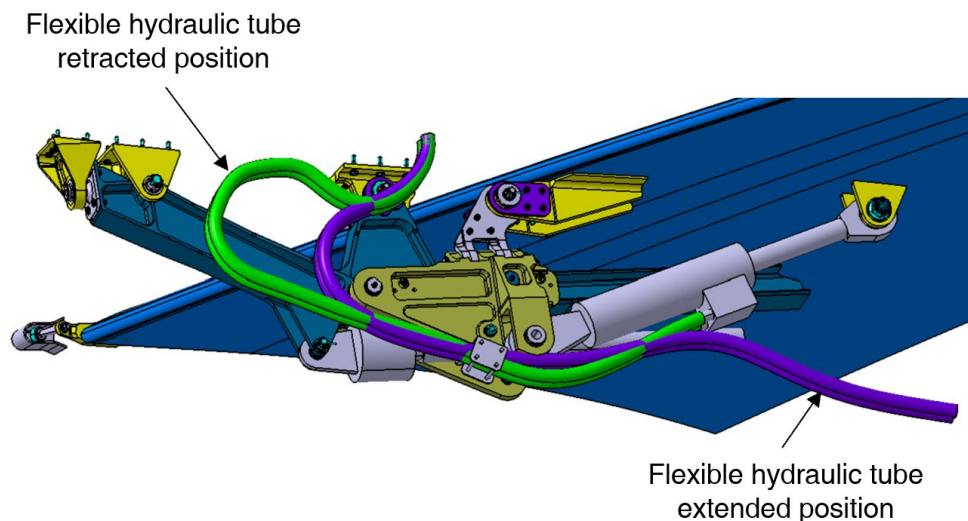


Figure 8 – Hydraulic flexible tube path and guidance options

#### 4.4 Redundancy

The airworthiness requirements for ailerons state that the control surface must be able to be actuated at any condition. To meet this requirement, in addition to the airworthiness requirements for high-lift devices, the following configuration is proposed (see Figure 9 below):

- Flap functionality:
  - State-of-the-art concept:
    - 2 support stations per flap (both linear driven)
    - Each ST consists of 1 Single Load Path (SLP) carriage, 1 SLP track and 1 back-to-back and thus Multiple Load Path (MLP) rear-link
  - MFFM concept:
    - 3 support stations (ST1 & ST3 are driven by a linear actuator)
    - Each ST consists of 1 SLP carriage, 1 SLP track and 1 MLP rotation actuator replacing a state-of-the-art rear link.
    - Skew sensors are needed on each station to monitor both the linear and the rotational movement differences between the 3 stations (integrated in the actuators or stand-alone systems).
- Aileron functionality:
  - State-of-the-art concept:
    - 1 rotation actuator attached to 2 different hydraulic power units
  - MFFM concept:
    - 3 rotation actuators driven by 2 or 3 different hydraulic power units → compensating for the loss of 1 rotation actuator or power unit

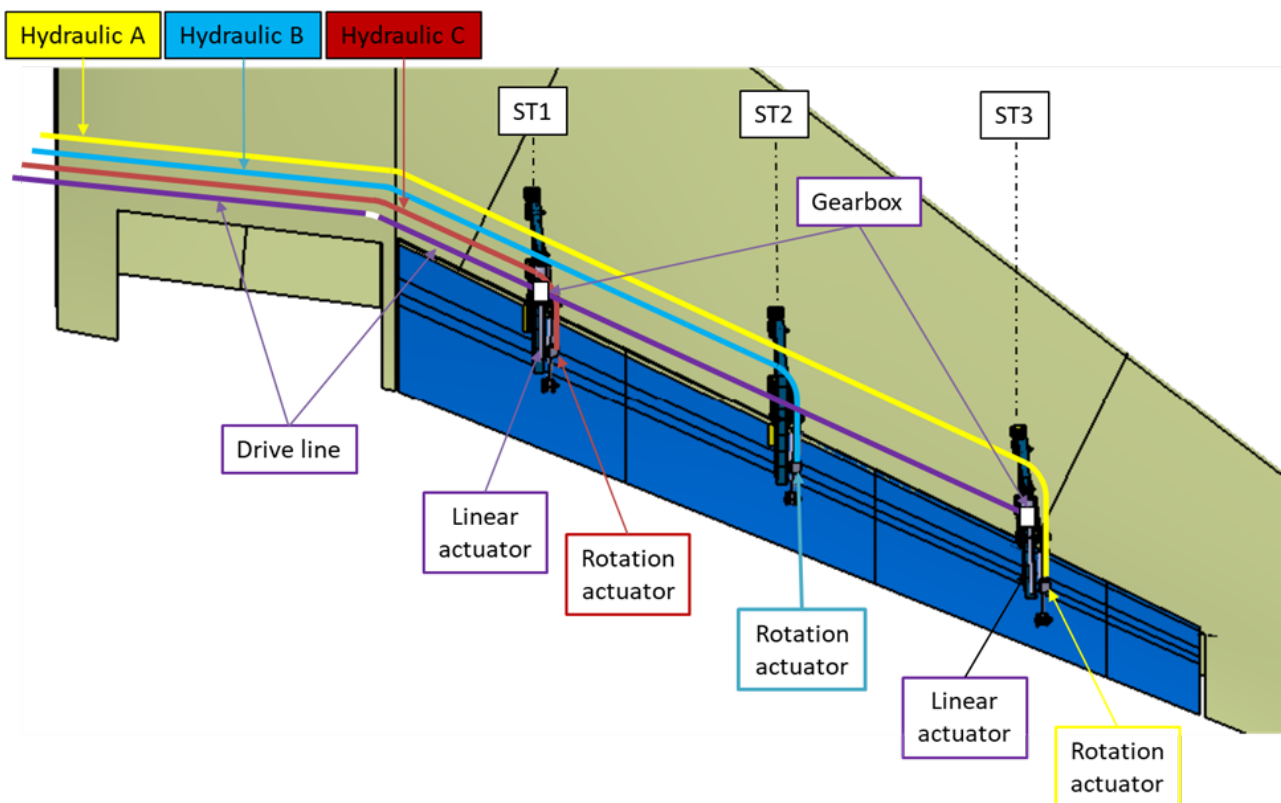


Figure 9 – Systems lay-out (redundancy) example

#### 4.5 Fairing concept

Same as on state-of-the-art aircraft, the flap supports are aerodynamically covered by means of fairings.

The fairing loft definition parameters used for the design are the following

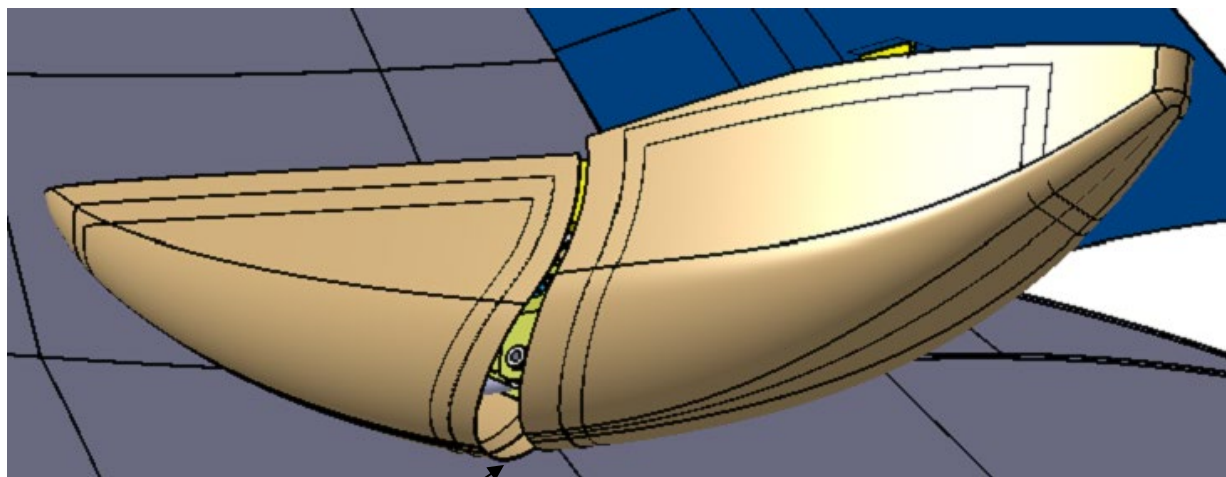
- Create a low drag cover around the track support mechanism with sufficient internal clearance to allow all the necessary movements – *proven design*
- Choose split line and rotation axis of the moveable fairing to allow both up- and downward movements in any position – *novel design*
- Limit fairing length to fit under the flap

The split line and rotation axis definition is directly linked to the novel multi-functional flap kinematics and hence has been investigated in detail to come up with a suitable fairing kinematics solution as state-of-the-art fairing kinematics typically does not allow for an upward flap rotation.

The novel fairing lay-out consists of

- A fixed fairing rigidly attached to the track or wing
- A moveable fairing attached to the carriage, following the movement of the flap
- A rod connection between flap and moveable fairing to impose the fairing rotation

⇒ allowing the fairing to follow both upward and downward rotation of the flap



Split line opens at fairing  
bottom creating gap

Figure 10 – Fairing kinematic at retracted flap setting; rotated upwards

#### 4.6 Spoiler interaction

When the multi-functional flap is in its retracted position it is partly covered on top by spoilers (see Figure 11 below). If a roll manoeuvre needs to be performed, the multi-functional flap will rotate upwards at one side of the aircraft leading to a clash with the spoiler.

No solution for a direct mechanical link between both systems can be presented in this paper. Due to the complexity of the combination of a fixed (spoiler) and a moveable (multi-functional flap) system which both are driven with separate actuation systems, there is no straight-forward solution. At this moment, the proposal would be to actuate the spoiler to the needed angle when the multi-functional flap is rotated upwards, avoiding a collision.

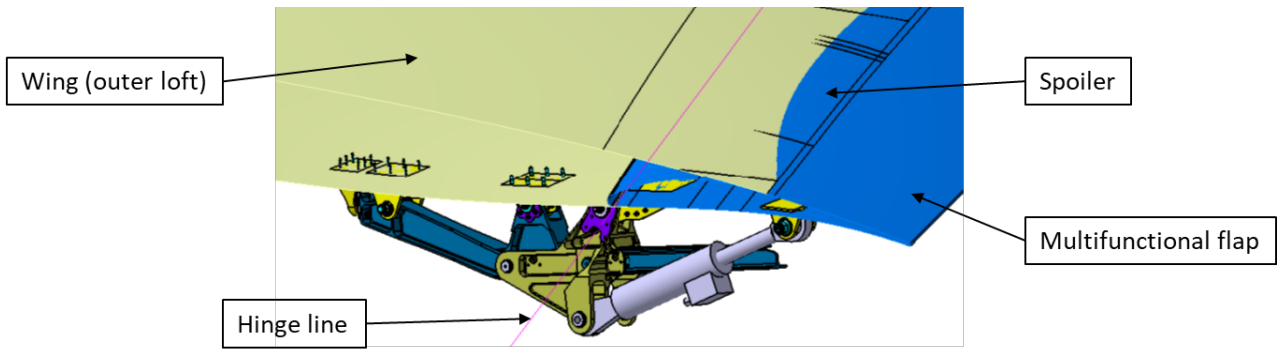


Figure 11 – Multi-functional flap - spoiler interface

### 5. Aerodynamic assessment and potential for load alleviation

In order to give insight into the aerodynamics of the HSBJ high-lift system, its novel wing layout and the multi-functional flap, the DLR is performing a number of CFD studies with these new concepts.

The studies carry on the initial aerodynamic studies from TU Delft and feature highly-accurate Reynolds-averaged Navier-Stokes (RANS) simulations for edge-of-the-envelope flight conditions for the high-lift system. The aerodynamic simulations aim to ensure the same flight and handling qualities for the new layout, to understand its characteristics and to look at the behavior for higher angles of attack at the maximum lift coefficient  $C_{L,max}$ .

The CFD computations are performed using the DLR in-house RANS solver TAU [3] and CFD framework FlowSim [4], which allow a high accuracy with low computation times and many possible adaptations in the simulation to address the regions of interest for static and dynamic load cases. The simulations were made on a grid with 70 million points, a multigrid scheme for lowered computation times and the Spalart-Allmaras negative turbulence model [5].

The simulations include the fuselage, the complete wing and the high-lift system with the MFFM, however, engine nacelle, flap track fairings and tail plane are not included, therefore the absolute coefficients are not directly comparable to a reference configuration. Mach number studies are performed for  $Ma$  of 0.16 to 0.3 and Reynolds numbers of 16 to 30 million, respectively.

In Figure 12 a variation of angle of attack for the lift and drag coefficient of the HSBJ with the new wing layout in high-lift configuration is shown for  $Ma = 0.24$ ,  $Re = 24$  million and ground level flight conditions.

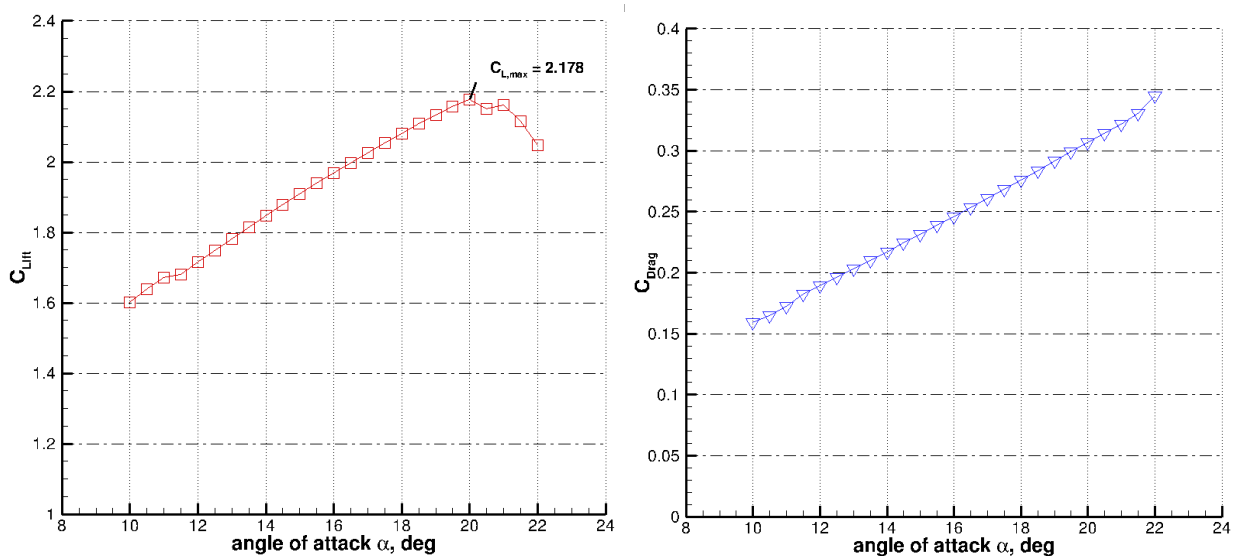


Figure 12 - Lift and Drag Coefficient for the HSBJ high-lift configuration for a Mach number of 0.24 and a Reynolds number of 24 million for an angle of attack sweep from  $\alpha = 10^\circ$  to  $\alpha = 22^\circ$

The constant climb of the lift coefficient with the increasing angle of attack shows a very suitable behavior for take-off and landing with the new wing layout and high-lift design. The high-lift system shows a very smooth course up to an angle of attack of 20°, where it reaches its maximum lift coefficient of  $C_{L,max} = 2.178$ . After its peak, the configuration shows a good stalling behavior, since it drops down moderately to a  $C_{L,max} = 2.04$  at 22° angle of attack. The drag coefficient indicates smooth flight characteristics for the high-lift system, since the drag coefficient rises constantly and predictably with the higher angles of attack, without having any swings at the examined angles of attack. Only at  $\alpha = 22^\circ$  the drag rises nonlinear, but this is expectable due to the stalling of the wing in this region. The figures show, that the high-lift system with the new wing layout shows a very smooth behavior for the overall values of lift and drag, even at a higher Mach number of 0.24.

In Figure 13 the pressure distributions for a Mach number of 0.2 and a Reynolds number of 20 million at three different spanwise locations of  $\eta=0.25, 0.4$  and  $0.7$  are shown, whereas  $\eta$  is the ratio of the y-location to the half-span width of 12.6 m for the HSBJ. The pressure distributions are then shown for 4 angles of attack, ranging from 14° to 20° and the first section is on the inboard flap, the other two are located on the outboard flap. It must be noted that the exact position and the size of the wing sections is not shown and the absolute  $c_p$ -values of each section are independent from each other.

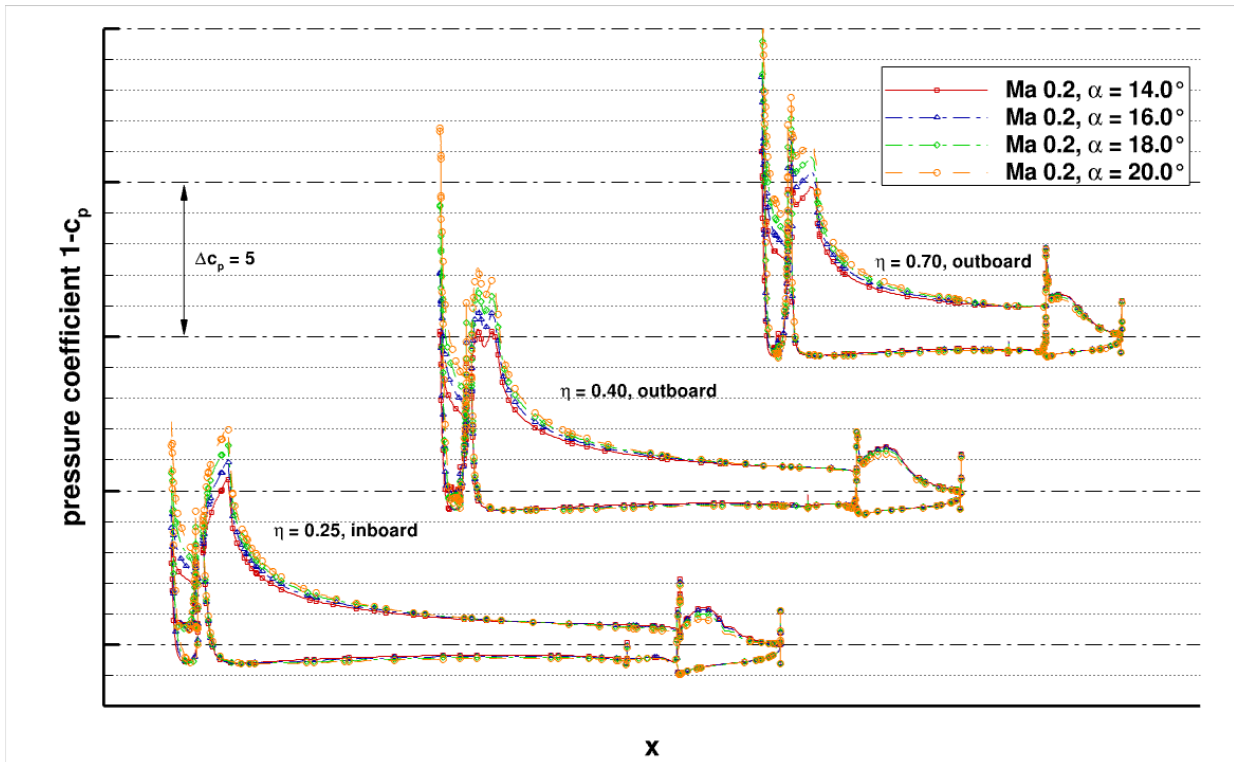


Figure 13 – Pressure distribution on 3 different sections of the wing at  $\eta=0.25, 0.4$  and  $0.7$  for Mach 0.2 at different angles of attack  $\alpha$

First, it can be seen that all sections show a very good aerodynamic behavior with increasing angle of attack. For the reference configuration, the maximum lift coefficient of  $C_{L,max}=1.86$  was estimated at an angle of attack of 19°. Since pylon and the tail plane are not considered in the simulations, the values of the maximum lift are not directly comparable, but even to an angle of attack of 20° the change in  $c_p$  – distribution shows a very smooth transition for the inboard and outboard sections. The  $C_{L,max}$  hereby reaches values of 2.16 for the new layout, however, this value must first be examined with an integrated nacelle and a tail plane. The pressure distribution is similar for all angles of attack, but the increase of  $\alpha$  leads to a lowered pressure on the upper surface and increases the overall loads, especially on the main wing and flap section. The biggest difference can be seen on the flow around the slat, which has an increased flow velocity on the upper surface and thus leads to higher loads on the leading edge of the main wing. The flap is hereby for all three sections mainly unaffected, which indicates stable aerodynamics for load control in this area.

In Figure 14 the spanwise vertical loads are depicted for the same load cases as in the previous figure. The main section in the top shows the overall forces for the total wing, with the slats and the flaps included. The bottom section only shows the part of the inboard flap up to span of  $\eta=0.3$  and the outboard flap up to a span of  $\eta=0.78$ .

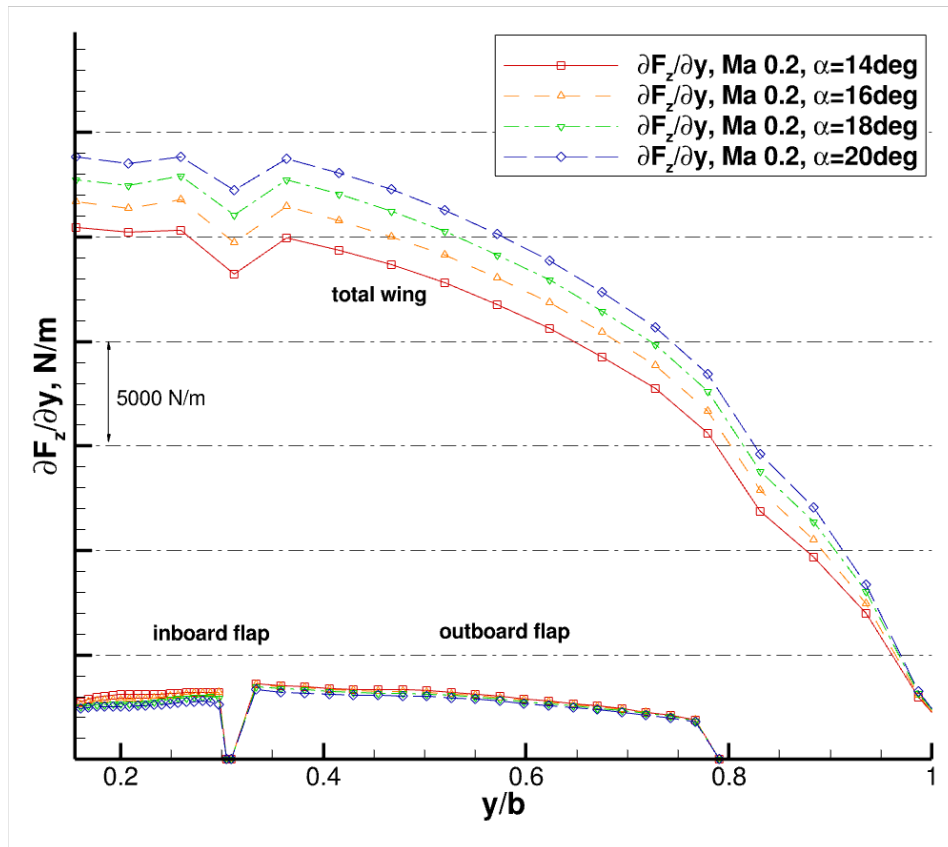


Figure 14 – Section cut loads in z-direction for Mach 0.2 and a Reynolds number of 20 million over the span for different angles of attack  $\alpha$

In general, the figure shows a preferable elliptical spanwise distribution of the loads on the HSBJ wing with the high-lift system. The loads on the section with the inboard and outboard flap are slightly increased and the flow stays attached at higher angles of attack on the outboard flap and the outer wing. Also, with an increase in angle of attack, as expected the overall sectional forces increase as well. However, as we have already seen in the previous case, the inboard and outboard flap are less affected by the angle of attack and even decrease slightly for higher angles. This shows that the higher angles of attack lead to stronger loads on front sections of the high-lift system. Nevertheless, both flaps have no flow separation for higher angles of attack and the strong loading of a flap is a good foundation for load control.

Since both flaps experience strong loads even for higher angles of attack and have a well attached flow, the second degree of freedom of the multi-functional flap is ideal for a usage in load alleviation cases. The size of the outboard flap, the new approach of the rotation after extension and the fast deflection speed are a substantial test case for load alleviation capabilities and need to be assessed in the future.

Therefore, in the next phase, the DLR will simulate and analyze the dynamic aerodynamics, on the one hand for the flap deflection with higher deflection speeds and on the other hand for gust load cases on the high-lift system. Thereby, the potential for load alleviation of the multi-functional flap on the wing can be analyzed and evaluated.

## 6. MFFM Test

### 6.1 Test Objectives

Demonstrate that it is possible to rotate a large control surface with representative stiffness and inertia at a speed of 60deg per second in retracted, take-off and landing flap positions, considering intact, actuator failure and jamming cases. While introducing simplified aero loading and simulating wing bending by moving the supports on the test rig.

Assess the effect of flap skew on actuator loading and compare with analytical results.

### 6.2 Simplifications

The full-scale flap body has been altered to be able to simplify the test setup without jeopardizing the test objectives and to reduce manufacturing cost of the test article.

The implemented changes are visualized in Figure 15 below and listed together with their justifications.

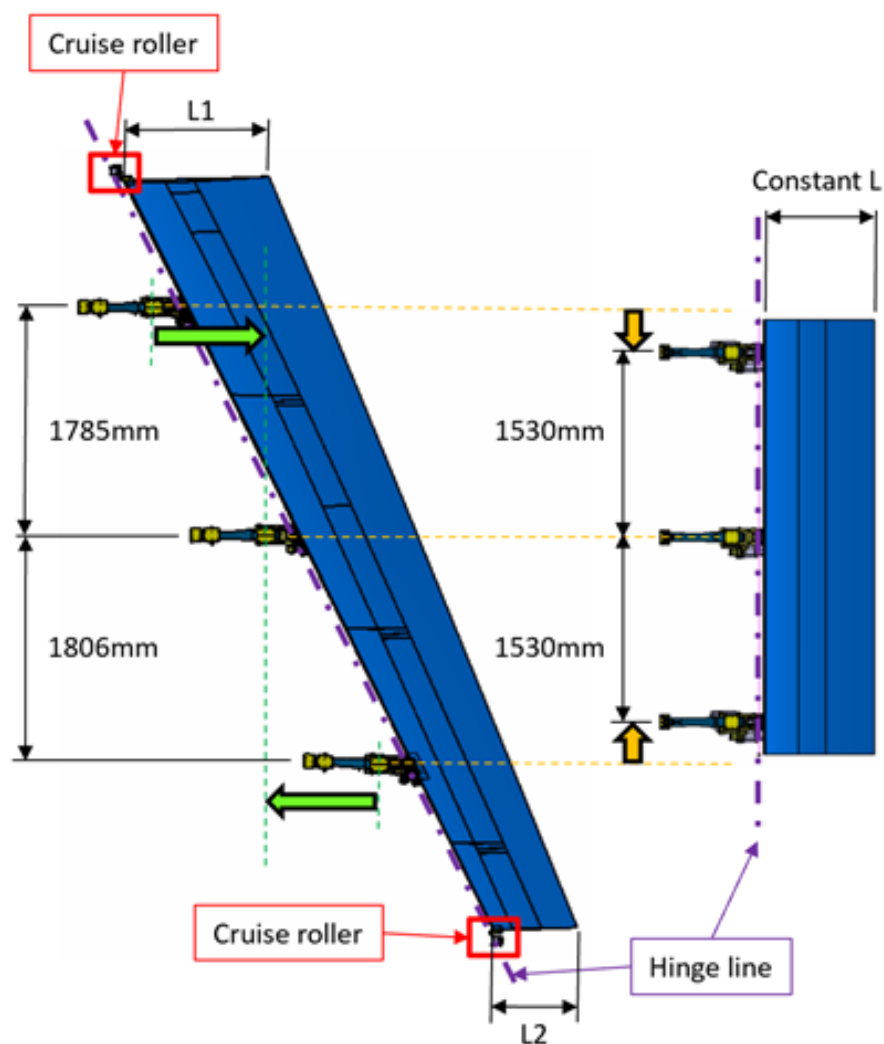


Figure 15 – Test simplifications

### 6.2.1 Tapered flap => rectangular flap + ST1 and ST3 in line with ST2 position

Following two simplifications change the typical out of plane flap motion into an in-plane flap rotation. (Figure 15):

- Change different flap chord lengths on each ST section to a constant chord length (=> constant flap section) for the entire flap
- Bring all 3 stations in line resulting in the hinge line being perpendicular to the station planes

Doing so gives as benefit:

- simplified load introduction (per station in 1 plane – no side load introduction needed)
- more compact test rig

### 6.2.2 Limiting the length of the flap

Other adaptations reducing the flap jig length and avoiding unneeded complexity are the following:

- bringing the flap stations closer to each other while keeping the original flap section
- eliminating the cruise rollers on both extremities of the flap allowing to cut of the flap at both ends just after ST1 and ST3

These changes aim to:

- reduce the needed space for the test rig
- Avoid unnecessary test (rig and test campaign) complexity due to the cruise rollers

Removing the cruise rollers has no detrimental effect on the test results. This is because the flap is already connected to the wing via 3 flap support stations, which transfer the wing bending towards the flap, resulting in a bending of the flap (and hence the hinge line). Having cruise rollers on the flap extremities will not change this flap bending significantly nor add additional effects on the hinge line.

## 6.3 Test setup

The MANTA MFFM demonstrator test article (Figure 16) which comprises; 3 flap supports, a rectangular flap, 3 identical rotation actuators, 2 dummy translation actuators; will be tested in a test rig which is built up from two modular track support test rigs designed and built at NLR, see Figure 17.

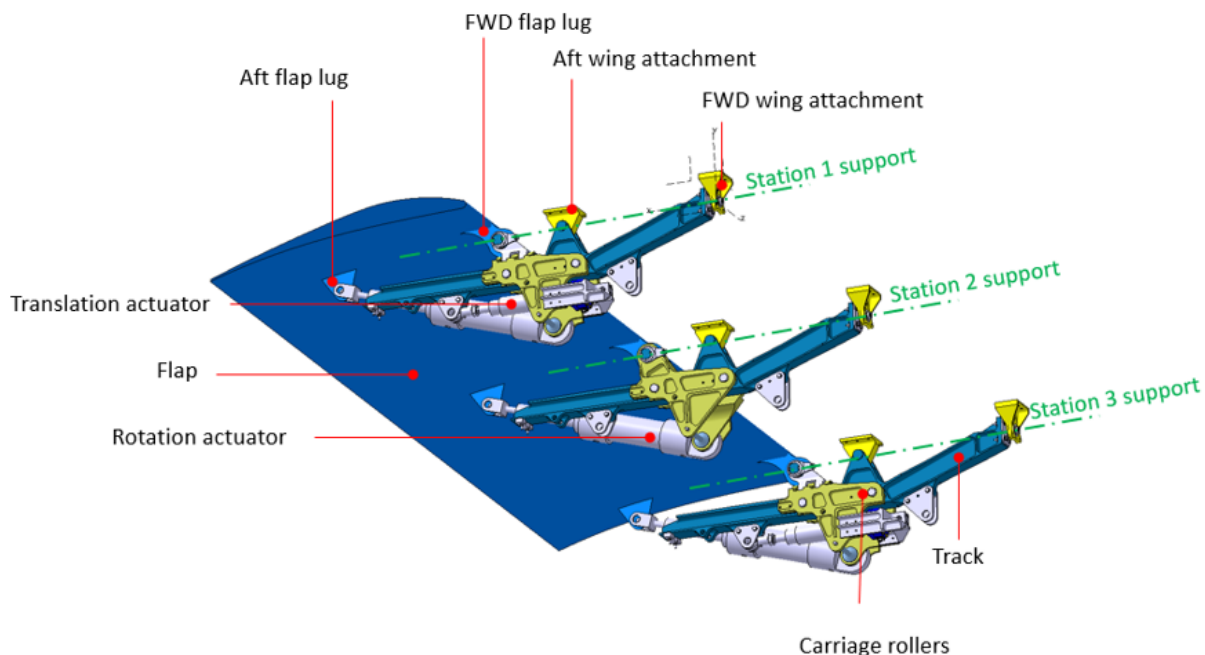


Figure 16 – MANTA MFFM demonstrator test article

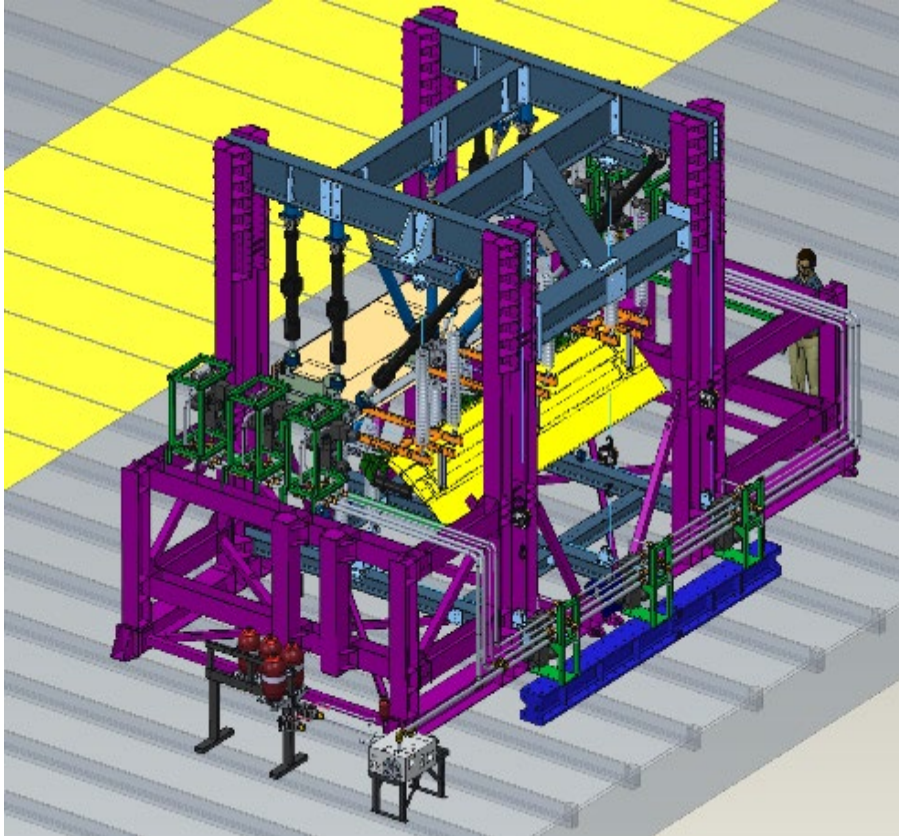


Figure 17 – MANTA test rig with MFFM installed

For MANTA MFFM functionality test the ‘wing bending displacement’ and ‘varying flap aero loads under flap rotation’ are applied for intact limit and failure ultimate load cases. The failure ultimate load cases simulate a disconnect in one of the rotation or translation actuators or a jamming of one of the carriages.

A realistic wing bending profile is replicated by introducing the corresponding displacements with 6 actuators at the two outer support stations (1 and 3) and constraining the support station 2 with struts. The flap aero loads are applied as simplified aero loads. One of the test rig design objectives is to mimic the changing aero load moments while controlling the flap with a rotation speed of 60 deg per second.

A sketch of the simplified aero Load Introduction Device (LID) with springs is given in Figure 18.

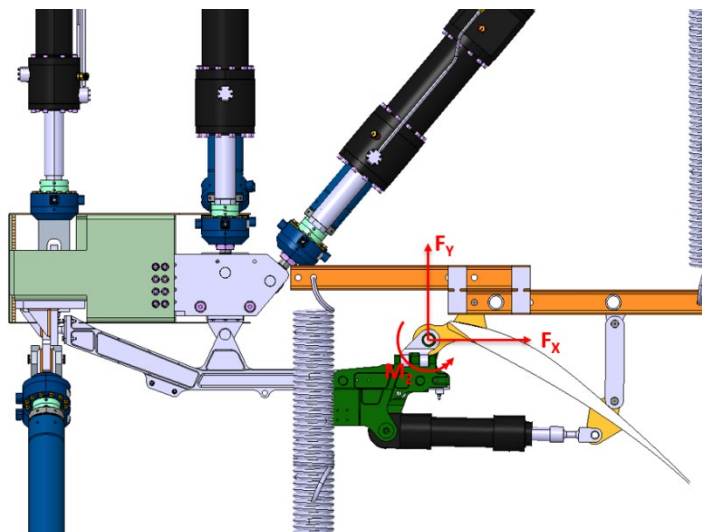


Figure 18 – Simplified aero load LID

## 7. Flexible tubing test

### 7.1 Test Objectives

The MANTA MFFM is equipped with flexible tubing to control the rotation actuators. A test setup is designed and built to demonstrate that it is possible to move the carriage 60.000 times from retracted position to full extension and back to retracted position without any damage or significant wear to the flexible hydraulic tubing. Specific measures are taken to test environmental temperatures and a constant pressure of 350bar in the hydraulic hoses.

### 7.2 Flexible hydraulic tubing test setup

Two (aerospace grade) flexible hydraulic hoses are connected to a hydraulic pump with reservoir to maintain a working pressure of 350bar in the hydraulic hoses. The hoses are installed into a customized test rig, designed and to be built at NLR, see Figure 19. A fixed hose end interface represents the wing connection and a moveable hose end interface represents the rotation actuator connection.

The test setup is suitable to simulate the flexible hydraulic hose movement from flap retracted position to full flap extension and back to retracted position, under environmental temperatures and working pressure.

The carriage movement will be applied with one actuator as depicted in Figure 19.

Cold temperature tests will be performed with a climate chamber installed around the flexible hose, to reach temperatures of -55degrees Celsius in the climate chamber.

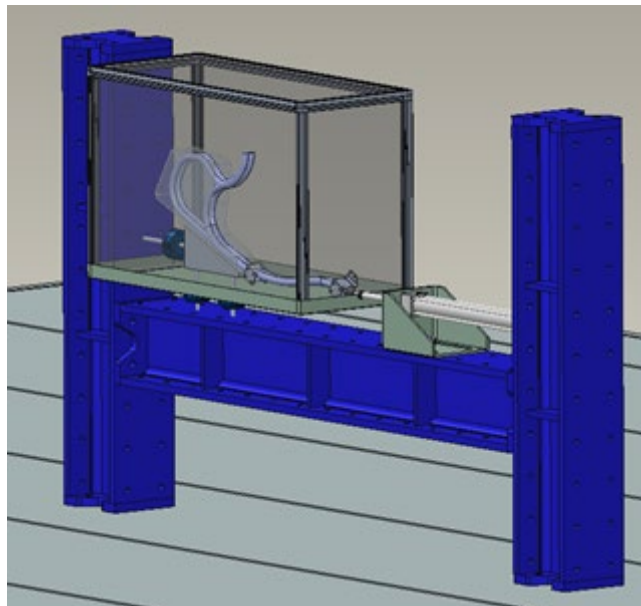


Figure 19 – Preliminary design of the flexible hydraulic tubing test setup

Regular stops are foreseen to perform visual inspections to detect potential damage and wear of hydraulic hoses, guide carrier and protection bracket.

## 8. Investigated opportunities

To optimize the weight even further and reduce maintenance cost, the following technologies are studied by the ADDIFLAP consortium:

- Titanium instead of Corrosion Resistant Steel roller track – traditionally this highly loaded part is made from corrosion resistant steel. The opportunity is studied to make the roller track out of titanium and use Wire Direct Energy Deposition method to create the raw material. Compared to traditional manufacturing, this technology allows for a more efficient material usage, reduces production waste and time-to-market. Nevertheless, high investment costs on equipment, building allowables and considerable deformation after printing are challenges that still need to be addressed.
- Sliding pads instead of rollers. A state-of-the-art carriage/rear link system relies on rollers to transfer loads from the flap panel via the roller track into the wing box. These rollers are part of the carriage assembly and need to be re-greased at regular intervals during the life of an aircraft. If the rollers could be replaced with sliding or rubbing pads which require no maintenance (other than inspection), this would reduce the direct maintenance cost by a non-negligible amount.

## 9. Conclusion

Combining load alleviation, roll control and high-lift functionalities into one large trailing edge control surface seems promising from a kinematics and aerodynamics perspective. Nevertheless, there are some design challenges to be addressed into detail, such as spoiler interaction and actuation control system design, these are out of the scope of the MANTA project.

Aerodynamic simulations demonstrate that the flow around the flaps show a good behavior for higher angles of attack and provide a good foundation for load alleviation and thereby roll control.

Two of the novel features of the MFFM concept, the rotation of the multi-functional flap at a maximum speed of 60degrees per second and the movement of the flexible tubing attached to the carriage, will be demonstrated via tests. Results are expected the first half of 2023.

Because of lack of weight data of the reference aircraft, the weight benefit is not quantified. However, through load alleviation on the wing root and elimination of a control surface (aileron), it is expected, the MFFM offers an overall weight benefit and performance improvement on aircraft level.

Next steps are to analyze the dynamic aerodynamics when the multi-functional flap is used as an aileron; and for gust load cases on the high-lift system. All results will be presented in one of the key deliverables of the MANTA project, the final synthesis report, due second half of 2023.

## 10. Acknowledgements

This work is carried out under the MANTA project, partly funded by the CS2JU through Grant Agreement n° 945521 [6]. The MANTA project is coordinated by Fokker Aerostructures B.V. (The Netherlands). Topic leaders are Airbus (Germany), Dassault Aviation (France) and SAAB (Sweden). Several novel control concepts are being developed and tested in the frame of MANTA. The MFFM presented in this paper is one of them.

Dassault Aviation (DAV) delivered a 3D model of the HSBJ wing and half fuselage to the MANTA consortium, together with reference data about the aircraft.

Dutch university TU Delft provided preliminary aero loading based on this input received from topic leader DAV.

The ADDIFLAP consortium, also funded by the CS2JU, consists of AIMEN (Spain), excellence research center for laser-based additive manufacturing processes and materials characterization and AC2T (Austria), excellence center for tribology activities. ADDIFLAP is studying the opportunities presented in section 8 with ASCO as topic leader.

## 11. Contact Author Email Address

mailto: [Marleen.Desmet@ascoindustries.com](mailto:Marleen.Desmet@ascoindustries.com)

mailto: [Ruben.Seidler@dlr.de](mailto:Ruben.Seidler@dlr.de)

mailto: [Jan.Docter@nlr.nl](mailto:Jan.Docter@nlr.nl)

## 12. Copyright Statement

The authors confirm that they, and/or their company or organization, hold copyright on all of the original material included in this paper. The authors also confirm that they have obtained permission, from the copyright holder of any third party material included in this paper, to publish it as part of their paper. The authors confirm that they give permission, or have obtained permission from the copyright holder of this paper, for the publication and distribution of this paper as part of the ICAS proceedings or as individual off-prints from the proceedings.

## References

- [1] <https://www.clean-aviation.eu/clean-sky-2/programme-overview-and-structure/high-level-objectives>
- [2] <https://www.asco.be/>
- [3] Gerhold, T., "Overview of the Hybrid RANS Code TAU," MEGAFLOW - Numerical Flow Simulation for Aircraft Design, edited by N. Kroll and J. K. Fassbender, Springer Berlin Heidelberg, Berlin, Heidelberg, 2005, pp. 81–92.
- [4] Meinel, Michael und Einarsson, Gunnar O. (2010) The FlowSimulator framework for massively parallel CFD applications. In: PARA 2010. PARA2010, 6.-9. Juni 2010, Reykjavik, Island.
- [5] Spalart, P., and Allmaras, S., "A One-equation Turbulence Model for Aerodynamic Flows," 30th Aerospace Sciences Meeting and Exhibit, 1992. doi:<https://doi.org/10.2514/6.1992-439>
- [6] GAM-2020-AIR – Number: 945521 "ITD AIRFRAME Grant Agreement for Members – Clean Sky 2 – Year 2020-2023 - Amendment 2"